Univerzita Karlova v Praze
Lékařská fakulta v Plzni

Autoreferát disertační práce

Morphological and genomic profiling of circulating tumor cells in metastatic colorectal cancer

Morfologická a genomická charakterizace cirkulujících nádorových buněk u metastatického kolorektálního karcinomu

Dipl. Biol. Jana-Aletta Thiele
Školitel: Mgr. Pavel Pitule, Ph.D.

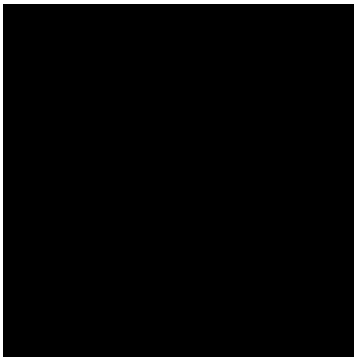

Plzeň 2018

Disertační práce byla vypracována v rámci doktorského studijního programu na **Ústavu Histologie a Embryologie** LF UK v Plzni.

Uchazeč: **Dipl. Biol. Jana-Aletta Thiele**

Školitel: **Mgr. Pavel Pitule, Ph.D.**

Konzultant: Prof. Dr. Peter Kuhn and Mgr. Pavel Ostašov, Ph.D.

Oponent 1: **Prof. Dr. rer. nat. Sabine Kasimir-Bauer**
Klinik für Frauenheilkunde und Geburtshilfe, Universitätsklinikum Essen
Hufelandstraße 55
45122 Essen, Germany

Oponent 2: **Doc. MUDr. Beatrice Mohelníková-Duchoňová, Ph.D**
Onkologická klinika, Fakultní nemocnice Olomouc
I.P. Pavlova 185/6, Nová Ulice, 779 00 Olomouc

Autoreferát byl rozeslán dne: ……..

Obhajoba disertační práce před komisí pro obhajobu disertačních prací studijního programu Anatomie, histologie a embryologie se koná dne: 14.09.2018

Místo obhajoby: Karlovarská 48, Plzeň, prostory Ústavu histologie a embryologie

S disertační prací je možno se seznámit na děkanátě Lékařské fakulty Univerzity Karlovy v Plzni, Husova 3, Plzeň.

Prof. MUDr. Milena Králíčková
předseda komise pro obhajobu disertačních prací v oboru Anatomie, histologie a embryologie.

Table of Contents

1 Abbreviations

5-FU	5-Fluorouracil
AJCC	American Joint Committee on Cancer
APC	Adenomatous-polyposis-coli
BRAF	V-Raf murine sarcoma viral oncogene homolog B
CA125	Cancer antigen 125
CDX2	Homeobox protein CDX-2
CEA	Carcinoembryonic antigen
CEC	Circulating endothelial cell
cfDNA	Cell-free DNA
CIMP	CpG island methylation phenotype
CIN	Chromosomal Instability
CK	Cytokeratin
CNV	Copy number variation
COI	Cell of interest
CRC	Colorectal Cancer
CT	Chemotherapy
CTC	Circulating Tumor Cell
CTCC	Circulating tumor cell clusters (two or more HD-CTCs)
CTC-cfDNA prod.	Probably apoptotic HD-CTC
CTC-LowCK	CTC with low or none CK signal
CTC-Small	CTC with a smaller nucleus
ctDNA	Circulating tumor DNA
EGFR	Epidermal growth factor receptor
EpCAM	Epithelial cell adhesion molecule
FDA	US Food and Drug Administration
FOBT	Fecal occult blood test
HD-CTC	Circulating tumor cell detected by the HD-SCA workflow
HD-SCA	High definition single cell analysis
lncRNA	Long non-coding RNA
LS	Lynch Syndrome
mAB	Monoclonal antibody
MMR	Mismatch repair
mRNA	Messenger RNA
MSI	Microsatellite Instability
MTsDNA	Multi-target stool DNA
NGS	Next generation sequencing
OS	Overall survival
PFS	Progression free survival
RBC	Red blood cell
RT	Radiotherapy
TE	Tris-EDTA
TNM	Tumor, nodes and metastasis (classification system)
Twist	Twist Basic Helix-Loop-Helix Transcription Factor 1
USC	University of Southern California
WBC	White blood cell
WGA	Whole genomes amplification

2 Introduction

2.1 Introduction to Colorectal Cancer

2.1.1 CRC Epidemiology

Within the European Union (EU) there were 1.373.500 new cancer related deaths expected for the year 2017 [1], with colorectal cancer (CRC) being the second most common cause of cancer death [2]. In the Czech Republic incidences of and mortality from CRC have been highest amongst Central and Western European countries ranking 4th worldwide for men and 16th for women [3]. After colonoscopy as the main early detection method has been introduced in 2002 a reduction of CRC incidence and mortality was observed [4, 5].

2.1.2 CRC Development

2.1.2.1 Molecular development of CRC

CRC develops through acquisition of multiple alterations in the genome. Mutations may add up, especially in highly mitotic tissues as the colonic epithelium [6]. Intestinal stem cells (ISCs) or differentiated cells in the colon epithelium have the potential to initiate CRC. Additional alterations are acquired over time, separating CRC into three phenotypes:

The Chromosomal Instability Phenotype

Genomic instability is a result of abnormal regulation of the mitotic spindle apparatus and repair mechanisms for double-strand DNA breaks [7]. One of the first steps of the chromosomal instability (CIN) pathway is the loss or inactivation of tumor suppressor genes like *APC* and *TP53* [8].

Microsatellite Instability Phenotype

In case that error occurs during cell replication and DNA polymerase fails to correct it, sections of DNA can be removed and repaired later by mismatch repair (MMR) proteins. Sometimes DNA polymerase stutter causes errors in areas of the genome with short tandem repetitions (microsatellites). These regions might change their

length resulting in microsatellite instability (MSI) [9]. Inactivation of MMR genes is caused either by somatic mutations or by abnormal DNA methylation [10]. The main MMR genes are MSH2, MSH6, PMS2 and MLH1. CRC is separated in categories with ≥30% instability, named MSI high (MSI-H) and MSI-low (MSI-L).

CpG island methylation phenotype

Epigenetic silencing through aberrant methylation of the promoter regions of a gene is as effective as a mutation of the DNA and can occur at cytosine bases [9]. Many are present in promoter regions of genes within repetitive sequences of the CG-dinucleotide (CpG-islands). CpG-island methylation in the promotor region leads to reduced gene expression or eventual silencing. One of the typical genes silenced, are members of the MMR system, resulting in similar changes as in case of MSI-H tumors, linking these two phenotypes together.

2.1.2.2 Hereditary predispositions for CRC

Lynch Syndrome (LS), also called HNPCC is characterized by a MSI-H phenotype, which is observed in 95% of these cases as a result of germline mutations in MMR family genes [11]. A common marker for LS is also a family history of CRC and a marker to distinguish sporadic CRC from LS is a mutation in BRAF, which is rare in LS, but common in sporadic, MSI-H tumors [12].

Familial adenomatous polyposis is associated with a heterozygous mutation of the tumor suppressor gene APC, which is known as the 'gatekeeper' of CRC [13]. It only accounts for 1% of all CRC and is typically clinically manifested by up to thousands of small adenomatous polyps that develop at an early age (15 to 35 years) [14].

2.1.3 Diagnostics of CRC

2.1.3.1 Diagnostic methods

Over 200.000 CRC patients per year die from CRC [15], regular screening for early diagnosis is essential as 5 year CRC survival chances drop from 90% for localized disease down to 12% for patients with distant metastasis [16]. The most frequent screening method for CRC is the analysis of stool for occult blood (fecal occult blood

test, FOBT). After implementation of FOBT in Europe a decrease in CRC mortality (15-33%, depending on the country) was observed [17].

2.1.3.2 Classification of CRC

The most commonly used staging method is the TNM system by the American Joint Committee on Cancer (AJCC) in which the letters are describing the primary tumor (T), spreading to lymph nodes (N) and probable spread to distant organs (metastasis, (M)). The official classification with description of all possible values for T, N and M are described in **Table 1.**

Table 1: TNM staging in colorectal cancer

Source: https://www.cancer.net/cancer-types/colorectal-cancer/stages

T0	There is no evidence of cancer in the colon or rectum.	**N0**	No spread to regional lymph nodes
Tis	Carcinoma in situ (Cancer cells are found only in the epithelium or lamina propria)	**N1a**	Tumor cells found in 1 regional lymph node
T1	The tumor has grown into the submucosa	**N1b**	There are tumor cells found in 2 to 3 regional lymph nodes
T2	The tumor has grown into the muscularis propria	**N2a**	There are tumor cells found in 4 to 6 regional lymph nodes
T3	The tumor has grown through the muscularis propria and into the subserosa	**N2b**	There are tumor cells found in 7 or more regional lymph nodes
T4a	The tumor has grown into the surface of the visceral peritoneum	**M0**	The cancer has not spread to a distant part of the body
T4b	The tumor has grown into or has attached to other organs or structures	**M1a**	The cancer has spread to 1 other part of the body beyond the colon or rectum
		M1b	The cancer has spread to more than 1 part of the body other than the colon or rectum.
		M1c	The cancer has spread to the peritoneal surface

An overall clinical stage is appointed taking the TNM classifications into consideration. Stages reach from 0 to IV, with higher numbers being associated with further advanced cancer.

2.1.3.3 Molecular markers for therapy decision

Levels of CRC markers like cancer antigen 125 (CA125) and carcinoembryonic antigen (CEA) are evaluated in blood serum [18, 19]. From solid biopsies of CRC tumors, the mutation status of the proto-oncogenes *KRAS* and *BRAF* are acquired, as they have been proven to be markers of resistance to anti-EGFR therapy [20].

2.1.4 Therapies for CRC

If the cancer has not spread to distant organs (M0), CRC is mainly treated with surgery in a curative intent [21]. In case of lymph node involvement (AJCC stage III) adjuvant (applied post resection) chemotherapy has proven to prolong overall survival (OS) [22]. For patients with stage IV CRC, surgery is still the only chance for a cure. Radiotherapy (RT) will contribute to shrinkage of the tumor and therefore support or facilitate complete tumor removal. The most common and successful CT for CRC is 5-Fluorouracil (5-FU). Also applied is platinum-based therapy. The two available targeted therapies against CRC are containing antibodies that recognize the vascular endothelial growth factor (VEGF) or the epidermal growth factor receptor (EGFR).

2.2 Introduction to circulating tumor cells

CTCs as fluid surrogates of dynamic tumor evolution in the blood could be valuable for the clinic. CTCs are cells with epithelial origin and possess biological and physical properties that enable their differentiation from surrounding blood cells. The most used markers to detect CTCs in the blood are the epithelium specific cell adhesion molecule EpCAM or cytokeratins. The proteomic profile of a CTC reflects the protein profile of the tissue from which it originated, as well as markers for treatment decisions (e.g. EGFR or HER2) [23, 24]. The size of CTCs is usually bigger as of the surrounding blood cells. Also, CTCs have a higher deformability the higher their metastatic potential but are in general less deformable than WBCs [25].

2.2.1 Dynamics of CTCs

The main and mostly accepted theory for active CTC migration is that the cells undergo epithelial-to-mesenchymal transition (EMT), loosing their junctions, adhesion to basal membrane, apical-basal polarity and change into an elongated cell with increased motility and invasive potential [26]. One trigger can be a tumors low oxygen supply (<40 mmHg). Transcription factors like ZEB1, FOXC2, TWIST, SNAIL and

SLUG responsible for EMT are activated [27, 28]. This leads to cell motility and invasive characteristics [29]. Protein expression for epithelial characteristics might be down regulated (cytokeratins) [30–33].

In contrast, the passive shedding of cells into the vasculature through parts of the tumor breaking off is supported by pathologists observations of tumors growing inside blood vessels [34, 35]. It is even suspected that circulating tumor cell clusters (CTCCs), may get stuck in small capillaries, which could eventually support metastasation [36]. To establish a distant metastasis, a CTC has to extravasate the vasculature and start to proliferate at a distant site. This process was proposed as mesenchymal-to-epithelial transition (MET) [26]. Key proteins in MET include cell adhesion molecules (CAMs) and all proteins supporting epithelial state (like E-cadherin and β-catenin) [37].

2.2.3 Methods to detect and capture CTCs

Only one CTC detection system is approved by the EU and the FDA, the CELLSEARCH® system (Veridex, Warren, USA). EpCAM expressing cells are magnetically separated from leukocytes and then stained with anti CK antibodies (CK8, CK18, CK19), anti CD45 (a specific leukocyte antibody) and the nucleic acid stain DAPI. CTCs are defined as EpCAM expressing cells that have a nucleus ($DAPI^{pos}$), are CK^{pos} and $CD45^{neg}$ [38]. Other CTC detection techniques have been developed, but the majority is utilizing EpCAM for detection and enrichment of CTCs [39].

Another method is the depletion of leukocytes after RBC lysis. Others use differing density of CTCs [40], or make use of the differing size of CTCs and WBCs [41]. One strategy avoids pre-selection of a cell population carrying a specific marker, the high definition single cell analysis (HD-SCA) platform (Epic Sciences, San Diego, USA) [42].

2.2.4 Downstream characterization of CTCs

CTCs could be analyzed through next generation sequencing for therapy relevant markers like *KRAS* mutation status. A changing mutation status in CTCs compared to

the mutation status in the primary tumor could enable a switch to more appropriate treatment and save time for the patient [43, 44].

3 Goals and hypotheses

3.1 Enumeration of CTCs in CRC

Our goal was to enumerate all CTCs using the HD-SCA workflow and determine a subcategory of CTCs based on morphologic heterogeneity associated with survival and/or metastasis. Also, we planned to analyze CTCCs to evaluate their potential as unique indicators of disease progression:

Hypothesis 1: It will be possible to distinguish different subsets of CTCs by morphological characteristics.

Hypothesis 2: One or more of the classified CTC categories will be associated to survival.

3.2 Copy number variation profiles of CTCs in CRC

The molecular analysis of CTCs has been demonstrated to provide more information and a novel source of predictive potential. Using the HD-SCA workflow it has already been shown that multiple clones can exist within the CTCs of one prostate cancer patient [45]. So far CNV profiles of single CTCs of CRC patients have not been analyzed.

Our goal was to observe clonality within the CTCs of our CRC cohort and to compare detected clones with those of the individual cells extracted from corresponding tissue samples to monitor a clonal evolution of the cancer in the blood of a CRC patient:

Hypothesis 3: We will observe CNV clonality within CTCs of CRC patients and at least one clone will be associated to survival.

Hypothesis 4: A detected clone within CTCs will abe discovered in the individual cells of corresponding tumor tissue of the primary tumor or the liver metastasis and therefore be proof of tumor evolution and descent of CTCs in CRC.

4 Materials and methods

Collaboration with Dr. Peter Kuhn at University of Southern California (USC) allowed implementation of major parts of the High-Definition Single-Cell Analysis (HD-SCA) workflow in the Laboratory of Tumor Biology at the Faculty of Medicine in Pilsen. The method has been described by Marrinucci et al. in 2012 [42].

4.1 Blood sample collection and processing

In this prospective study 47 patients from the Czech Republic with clinically confirmed CRC in AJCC stage IV were analyzed. Additionally, the blood from ten healthy donors has been drawn and analyzed. An overview of cohort characteristics is presented in **Table 2**.

Table 2: Patient cohort characteristics

Category	Groups	No.	%
Gender	male	25	53.2
	female	22	46.8
Age	30-50	5	10.6
	50-70	30	63.8
	>70	12	25.5
CRC Location	Left	29	61.7
	Right	10	21.3
	Transvers	7	14.9
	Left & Right	1	2.1
Synchronous Disease	Yes	30	63.8
	No	16	34.0
	N.A.	1	2.1

Blood samples were collected before surgery and a follow up blood draw within two weeks up to 5 months after surgery through a peripheral blood draw. During patient's surgery, also a piece of resected tissue was slightly touched on a standard microscopy slide (touch prep). This slight contact left an imprint of a single cell layer

of the tissue on the slide. These slides were treated like blood preparation slides, but were imaged manually.

Red blood cell lysis was performed, and then WBC count determined using a Buerker chamber. 3 million cells per slide were plated. Cell suspension was added to custom made Marienfeld adhesive slides and treated with 7% bovine serum albumin (BSA). Slides were cover slipped and wrapped in aluminum foil and stored at -80°C.

4.2 Fluorescent staining and slide imaging

Microscopy slides were thawed and treated with 2% PFA (paraformaldehyde), ice cold methanol, 10% goat serum and then stained for 40 min with anti-pan-cytokeratin and conjugated antibody against CD45 in dilution. Then secondary antibody was applied for 20 min containing Alexa Fluor® 555 IgG1 and DAPI. Slides were washed in 1X PBS twice and 110 µl live cell mounting medium (0.05 g n-propyl gallate, 0.26 g Tris-HCl and 8 ml of ddH_2O were mixed; 4 ml of that solution were added to 36 ml glycerol) were distributed evenly over the active area of the slide and coverslip mounted without bubbles. A custom configured, fully automated epifluorescent microscopy system was used for imaging with a 10X objective lens, a calibrated and automated x-y-z-stage and a control board integrating all components. The software used DAPI images to set focus, then 6912 digital images were taken for each slide. Cells were annotated with a cell ID and Cartesian coordinates.

4.3 Technical analysis of COIs

The custom imaging analysis software uses algorithms for the detection of COIs considering the signal of cytokeratin (CK), CD45 and DAPI. COI subcategories were defined by the following characteristics:

- HD-CTC: CK^{pos}, $CD45^{neg}$, and distinct nucleus
- CTC-LowCK: $CK^{low/neg}$, $CD45^{neg}$, and distinct nucleus

- CTC-Small: CK^{pos}, $CD45^{neg}$, with small and round nucleus
- CTC-cfDNA producing: CK^{pos}, $CD45^{neg}$, and shredded or minimized nucleus.
- CTCCs: clusters of two or more HD-CTCs

4.4 Single cell isolation and library construction

For isolation of single-cells from a microscopy slide, a fluorescence microscope was used (Olympus IX81) in combination with a micromanipulator (TransferMan® 4r, Eppendorf) and the imaging software ImagePro.

For whole genome amplification (WGA), the GenomePlex® Single Cell Whole Genome Amplification Kit (WGA4, Sigma-Aldrich) was used. The QIAquick PCR Purification kit (Qiagen, Germany) was used according to manufacturer‘s instructions. DNA samples were quantified using the Qubit™ dsDNA HS Assay Kit (ThermoFisher Scientific, Germany). DNA concentrations were saved in a database and all samples were diluted to the same initial amount of 185 ng DNA in 55.5 µl total volume.

All samples were sonicated to a fragment size of 200 -250 bp. The NebNext®Ultra DNA Library Prep kit for Illumina® (New England BioLabs Inc.) was used in combination. All libraries were pooled at a final concentration of 10 mM using a volume of 5 µl/sample.

4.5 Sequencing and Single-Cell CNV analysis

Protocols for next generation-sequencing are in detail described in Baslan et al. [46]. The DNA libraries were sequenced on the HiSeq2500 (Illumina, USA) platform using a single end read 50 base pair protocol (SR50). To visualize similarities, a custom software tool was used and heatmaps were generated using cluster method ‚ward.D‘ and distance method ‚manhattan‘. A data resolution of 5k bins and a threshold of at least 50.000 bin counts was applied for inclusion of data.

4.6 Statistical methods used for CTC data

For analysis of the association of CTCs with OS and PFS, univariable Cox proportional hazards model was used for continuous variables including hazard rate calculations and visualized with Kaplan-Meier survival estimation plots. For binary variables, Kaplan-Meier survival estimates in combination with significance tests (Gehan Wilcox, log-rank) were calculated. Categorical variables have been tested through contingency tables with either Chi-square test or Fisher's exact test. For the associations between categorical and ordinal or quantitative variables, Mann Whitney U test or Kruskal-Wallis ANOVA (depending on the number of categories) was utilized. Spearman's correlation has been applied to test associations between two ordinal or quantitative variables. All reported p-values are two-tailed and the level of statistical significance was set at $\alpha = 0.05$. Statistical analysis was performed in Statistica (ver. 12 Cz, TIBCO Software Inc., Palo Alto, CA, USA).

5 Results

5.1 Phenotypic and morphological heterogeneity within CTCs of CRC patients

86 blood samples of 47 CRC patients and 10 blood samples of 10 healthy volunteers were analyzed. Morphological heterogeneity was observed within the detected cells. HD-CTCs were often elongated or elliptical but also round (as seen in **Figure 1a**) with many HD-CTCs having appendix-like cytoplasmic projections. The size of HD-CTCs varied, the shape of the nuclei in HD-CTCs is often elongated or egg-shaped. The nuclear size of CTC-Small cells is comparable to nuclei of surrounding WBCs (**Figure 1c**). Also the nuclei of CTC-Small possess highest detected nuclear roundness (**Figure 2a**).

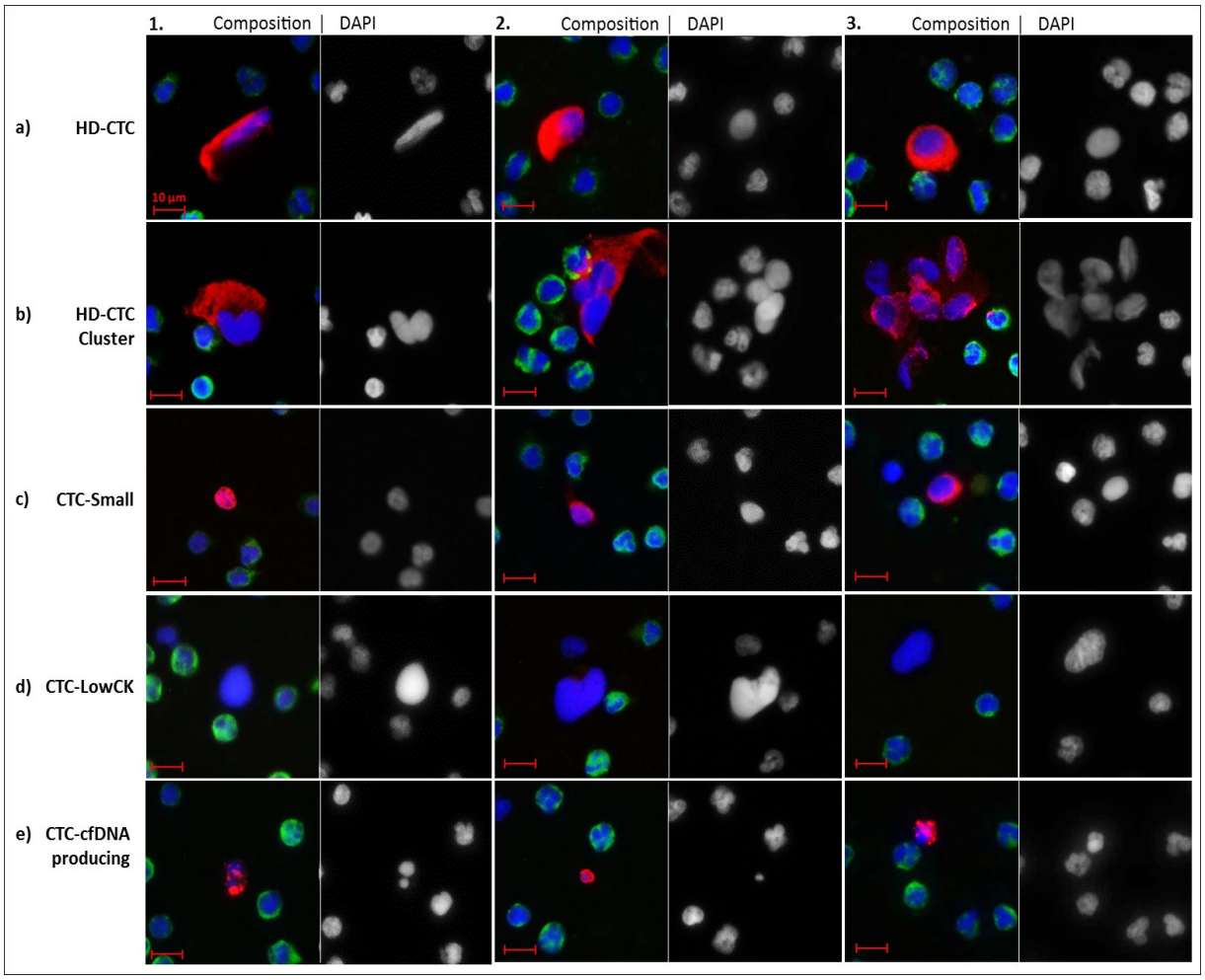

Figure 1: Heterogeneity within CTCs in CRC patients of the Czech Republic. Row **a)** shows a variation within the HD-CTC category of cells with an enlarged nucleus compared to WBCs and a CK^{pos} and $CD45^{neg}$ signal. Row **b)** displays clusters from two CTCs up to over 6 cells. In row **c)** are CTC-Small cells. Row **d)** displays COIs with low to no CK signal, $CD45^{neg}$ signal and enlarged nucleus. In row **e)** are the CTCs undergoing apoptosis and releasing cell free DNA. The red scale bars equal 10 µm. Parts of this figure have been published in Thiele et al.[47].

HD-CTCs had a mean nuclear roundness of 0.7, CTC-Small cells in contrast are more round with a median of 0.8. CTC-LowCK cells have a nucleus similar shaped as HD-CTC's nucleus, but the nuclear area is more than double the size with a mean of 356.5 compared to 158 in case of HD-CTCs. Measurements for all COIs are shown in **Figure 2**. The group of CTC-LowCKs shows enlarged nuclei, overall with a larger nuclear area than all other CTC cell types (**Figure 2b**). Besides single HD-CTCs, CTCCs were observed. These clusters were composed of at least two and up to 21 HD-CTCs in the largest observed cluster. The large heterogeneity of clusters is illustrated in **Figure 1b**.

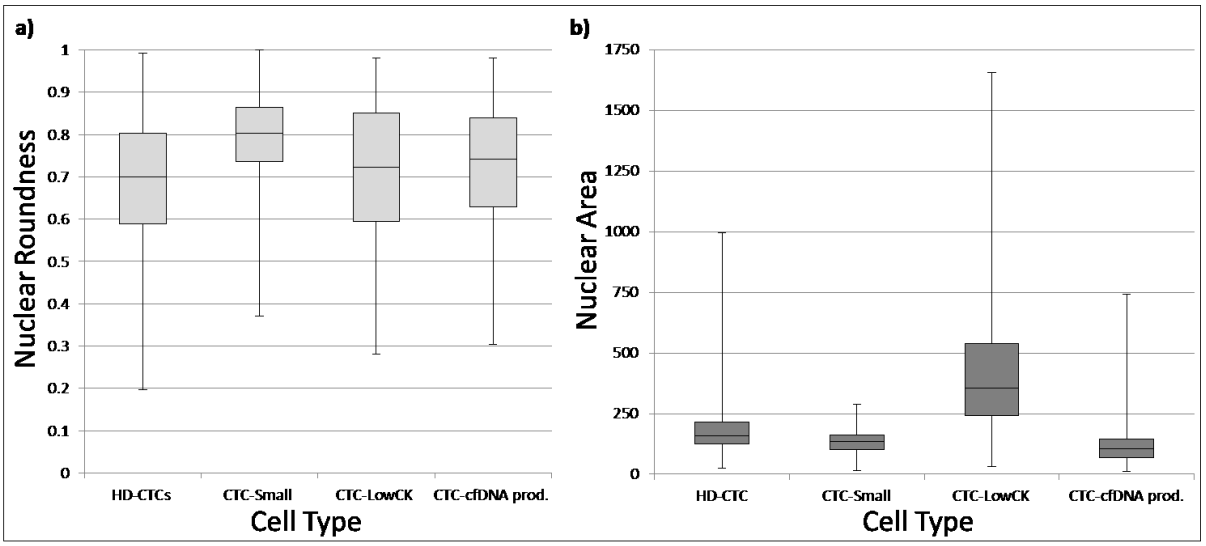

Figure 2: Nuclear Roundness and nuclear area of detected COIs. A total of 3001 HD-CTCs, 842 CTC-Small, 623 CTC-LowCK and 327 CTC-cfDNA producing cells have been analyzed for **a)** nuclear roundness. Nuclear roundness has been calculated as: 4x [signal area]/π x [major axis]^2. For CTC-cfDNA producing cells, the calculation for roundness is biased by the inability of the calculation to consider nuclear blebbing. **b)** Nuclear area is measured for all cell types in µm^2.

5.2 Evaluation of healthy donor samples

A total of ten healthy donors has been tested. Analysis resulted in a specificity of 100% for a cut-off of >3 HD-CTCs/ml blood. No clusters were detected in any of the healthy donors. Cut-offs for CTC-LowCK, to accomplish 100% specificity, were set at 8/ml, for CTC-Small as well and for CTC-cfDNA producing at 5/ml blood.

5.3 Enumeration data of HD-CTCs, CTC subcategories and CTCCs

For the pre-resection draws, 46 out of 47 were usable and only 39 patients out of 47 were available for follow-up draws.

5.3.1 Enumeration of HD-CTCs

Out of 46 patients, 24 had >3 HD-CTCs (52.2%) in the pre-resection draw. In the follow-up draw we detected >3 HD-CTCs in 20 (51.3%) patients. A comparison of average CTC counts/ml in the two blood draws per patient is shown in **Figure 3b** and

indicates a higher amount of total averaged HD-CTCs in the pre-resection draw (31.14/ml) compared to the follow-up draw (13.65/ml).

5.3.2 Enumeration of subcategories of CTCs

Average numbers/ml of the detected cells in CTC subcategories (shown in **Figure 3b**) dropped in the follow-up draw compared to the pre-resection draw for the CTC-Small and CTC-cfDNA producing cells. Using the threshold of >8 cells/ml blood, out of the 46 total pre-resection draws, 14 patients were positive for CTC-LowCK (30.4%) and 11 patients were positive for CTC-Small (23.9%). 13 patients showed >5 CTC-cfDNA producing cells (28.2%). In the follow-up draws from 39 patients, 12 had >8 CTC-LowCK/ml (30.8%), 11 had >8 CTC-Small/ml (28.2%) and 9 >5 CTC-cfDNA producing cells/ml (23.1%).

5.3.3 Enumeration of CTCCs

A total of 136 CTCCs were observed in the pre-resection draw across all patients. The distribution of cluster sizes within the pre-resection draws is displayed in **Figure 3a**. All CTCC size counts are lower in the follow-up draws. The calculations for average clusters/ml resulted in 4.2 for the pre-resection draw and a drop to 1.8 clusters/ml for the follow-up draws.

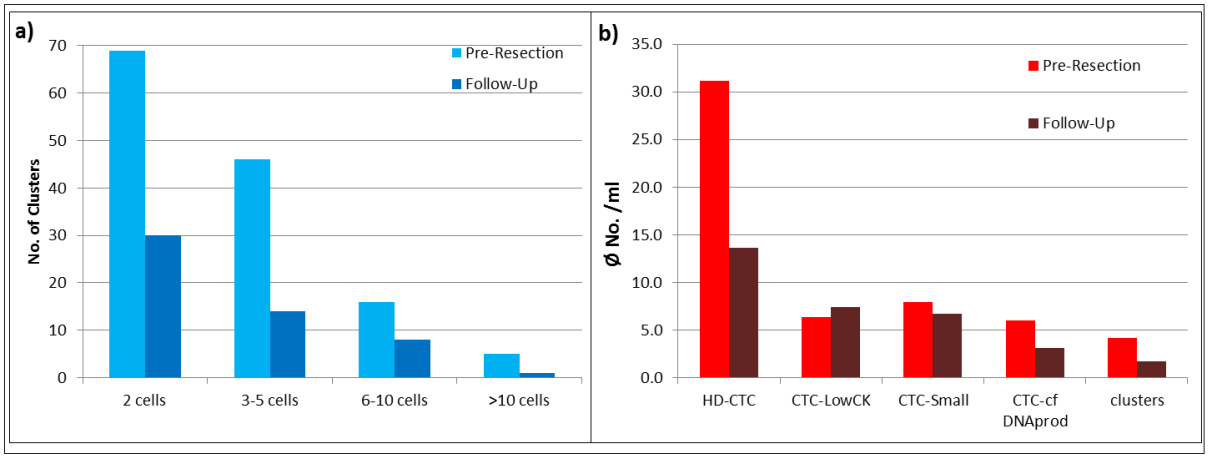

Figure 3: HD-CTC cluster sizes and average cell and cluster numbers for pre-resection and follow-up draws. Displayed are column diagrams of **a)** the distribution of total cluster counts (two analyzed slides/patient) sorted by cluster size (cell counts) for pre-resection and follow-up draw; **b)** total numbers of detected cell types/ml and clusters/ml blood in the entire CRC cohort for pre-resection and follow-up draws.

A draw was considered positive when at least one CTCC (=>2 HD-CTCs together) was detected. 18 patients (39.1%) were CTCC positive from the 46 pre-resection draws and 8 patients (20.5%) out of 39 were positive for clusters in the follow-up draw.

5.4 Associations of obtained data with survival

5.4.1 Association of clinical data with survival

Association between the location of the primary tumor and OS (p=0.030) and PFS (p=0.037) was found. Also we found an association between the size of the primary tumor and OS (p=0.002) and PFS (p=0.005). Kaplan-Meier curves for associations with OS are displayed in **Figure 4**.

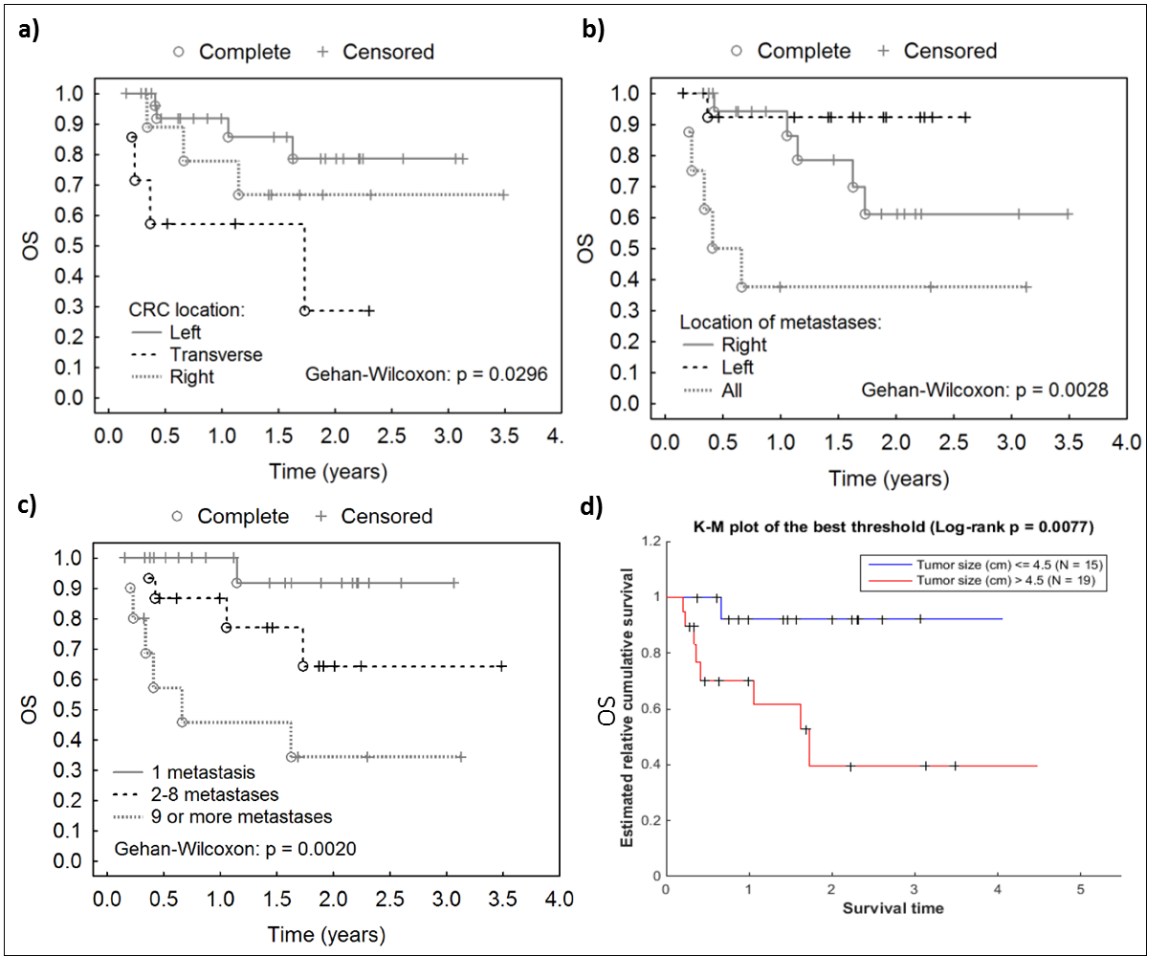

Figure 4: Kaplan-Meier curves for association between clinical cohort data and OS. a) Patients with left-sided CRC have the longest OS **b)** CRC patients with left-sided hepatic have the longest OS **c)** Patients with 9 or more hepatic metastases have the shortest OS. **d)** Optimized threshold for the tumor size shows a significant shorter OS for patients with primary tumors >4.5 cm.

For location of the primary tumor, patients with a left-sided CRC have the longest OS (**Figure 4a**), patients with transvers CRC the shortest OS. The OS of patients with hepatic metastases differs significantly between patients with metastases in the left side of the liver, the right side or all over the liver (**Figure 4b**) and statistics resulted in significant shorter OS the more metastases were observed (**Figure 4c**). Patients with primary tumors >4.5 cm have a significant shorter OS and PFS (**Figure 4d**).

5.4.2 Association of HD-CTC counts with survival

The enumeration data was analyzed for associations with OS and PFS without significant results.

5.4.3 Association of CTC subcategory counts with survival

CTC-Small/ml in the follow-up draw are associated with OS (p=0.040; Univariable Cox), with a HR=1.031. And 8 CTC-Small/ml blood are associated with PFS (p=0.015; Gehan-Wilcoxon).

5.4.4 Association of CTCCs with survival

Patients with CTCCs in the follow-up draw showed significant shorter OS (p=0.033; Gehan-Wilcoxon) and a Kaplan-Meier curve is presented in **Figure 5a**.

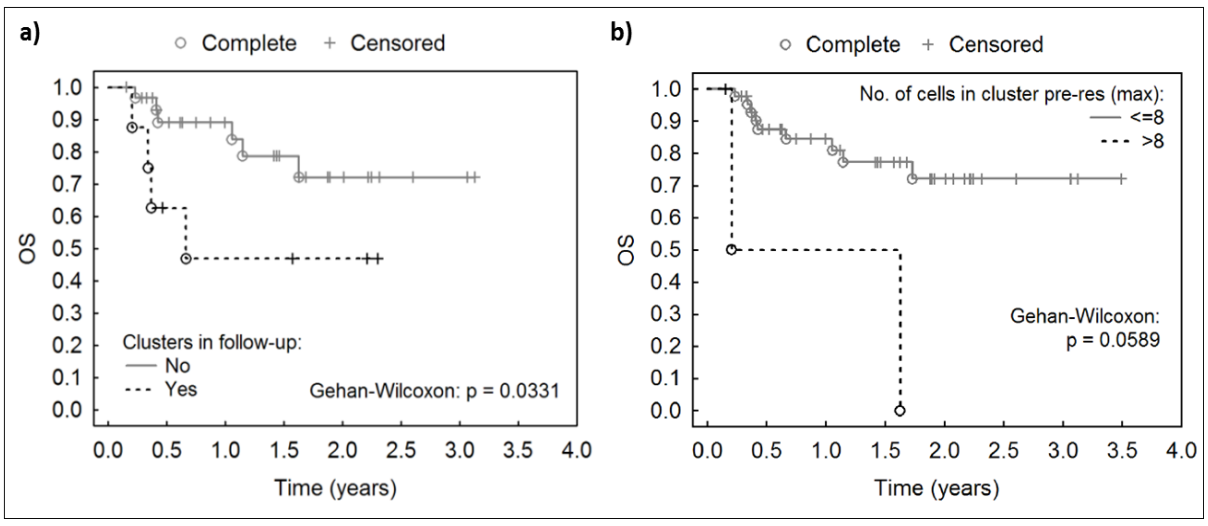

Figure 5: Association of CTCC variables with survival. a) Kaplan-Meier for the association CTCC positivity in the follow-up draw with OS **b)** Kaplan-Meier curve for the association of clusters containing >8 cells maximum in the pre-resection draws.

CTCCs/ml in the pre-resection draw were associated with OS (p=0.021; Univariable Cox). The Kaplan-Meier curve revealed that patients with CTCCs >8 cells detected in the pre-resection draw tend to have shorter OS (**Figure 5b**, p=0.059; Gehan-Wilcoxon).

5.5 Association of HD-CTC and CTCC enumeration data with clinical characteristics

5.5.1 Association of HD-CTCs counts with clinical characteristics

The obtained HD-CTC counts per ml blood in the pre-resection draw showed an association with the primary tumor locations (p=0.032; Kruskal-Wallis ANOVA) with highest amounts transverse tumors (**Figure 6a**). There was also a difference observed between *KRAS* wildtype and *KRAS* mutated primary tumors for HD-CTC/ml in pre-resection (p=0.003; Mann-Whitney U, **Figure 6b**). HD-CTC positivity (>3 HD-CTCs/ml) has also shown to be associated to *KRAS* status (p=0.027; Fisher's test).

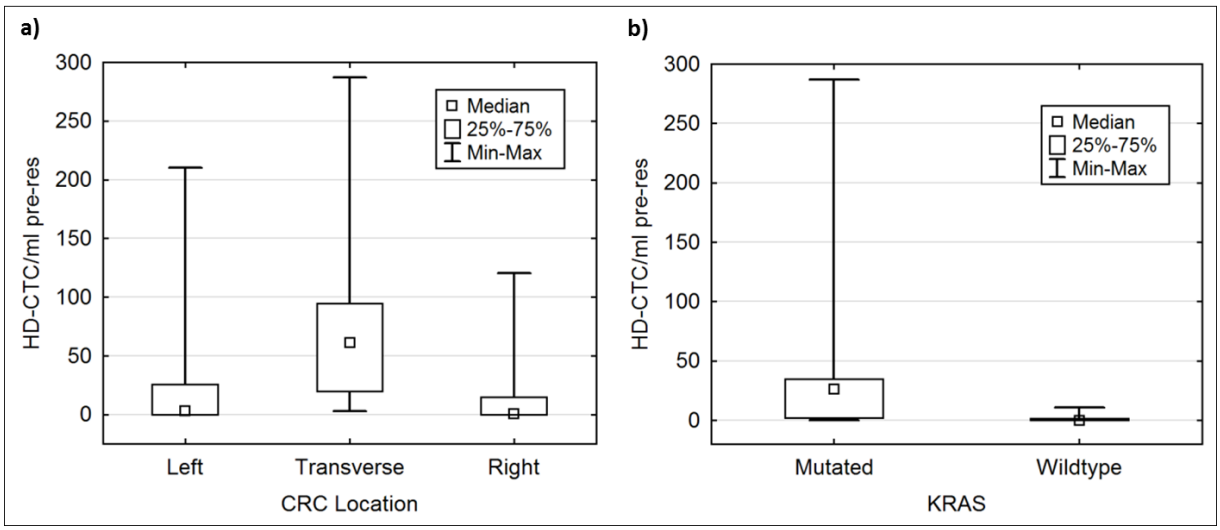

Figure 6: Association of HD-CTC counts in the pre-resection draw with tumor location and KRAS. Boxplot diagrams of **a)** HD-CTC/ml blood in the pre-resection draw in different primary tumor locations and **b)** HD-CTC/ml blood in patients with differing KRAS status.

The HD-CTC counts drop significantly after resection of the primary tumor compared to changes after resection of hepatic metastases (p=0.025; Chi-Square test).

5.5.2 Association of CTC subcategories with clinical characteristics

Counts of CTC-cfDNA producing/ml in the pre-resection are significantly higher the larger the hepatic metastases (p=0.032; Spearman's). For CTC-LowCK/ml in the pre-resection a significant varying number depending on the CRC location (p=0.038; Kruskal-Wallis) was detected. CTC-Small/ml blood in pre-resection draws differ significantly within patients with varying K*RAS* status (p=0.014; Mann-Whitney U).

5.5.3 Association of CTCCs with clinical characteristics

We detected a significantly higher average amount of cells within detected clusters in patients with M1 status at time of diagnosis (p=0.035; Mann-Whitney U, **Figure 7a**).

The amount of clusters/ml blood detected in the pre-resection draw was significantly higher in patients with *KRAS* mutated tumors (p=0.025; Mann-Whitney U, **Figure 7b**).

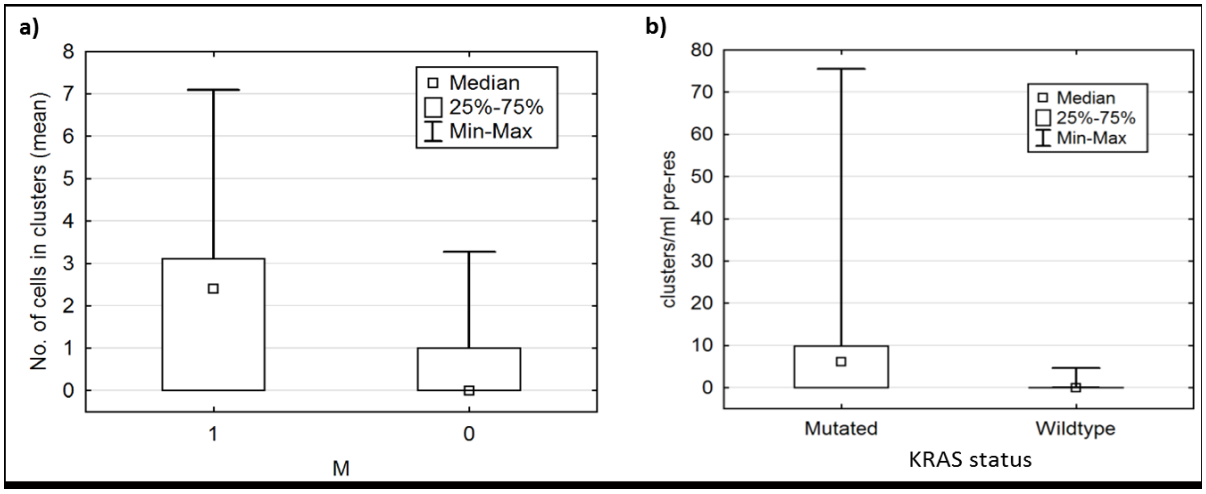

Figure 7: Association of CTCCs with metastasis and KRAS status. Displayed are boxplot diagrams of **a)** the mean no. of cells in clusters depending on M status; **b)** the amount of CTCCs/ml blood in the pre-resection draw depending on the *KRAS* status of the patient's CRC.

5.5.4 Mutual correlations between clinical characteristics

The size of the primary tumor has been associated to the number of hepatic metastases (p=0.044; Spearman), and the number of hepatic metastases was associated to their location (p=0.001; Kruskal-Wallis).

5.6 Analysis of CNV profiles from CTCs and tissue touch preps

No clonality was detected in a total of 136 analyzed HD-CTCs. Analysis of specific alterations resulted in the detection of 21.3% (29 HD-CTCs) of the cells with partly deleted or amplified Chromosomes.

We analyzed a total of 126 single-cells isolated from CRC touch preps of 12 patients from our cohort. Ten out of 12 patients (83.3%) showed clonal profiles within the analyzed cells (**Figure 8**). Out of the 126 isolated cells, 87 cells (69%) were part of clonal profiles.

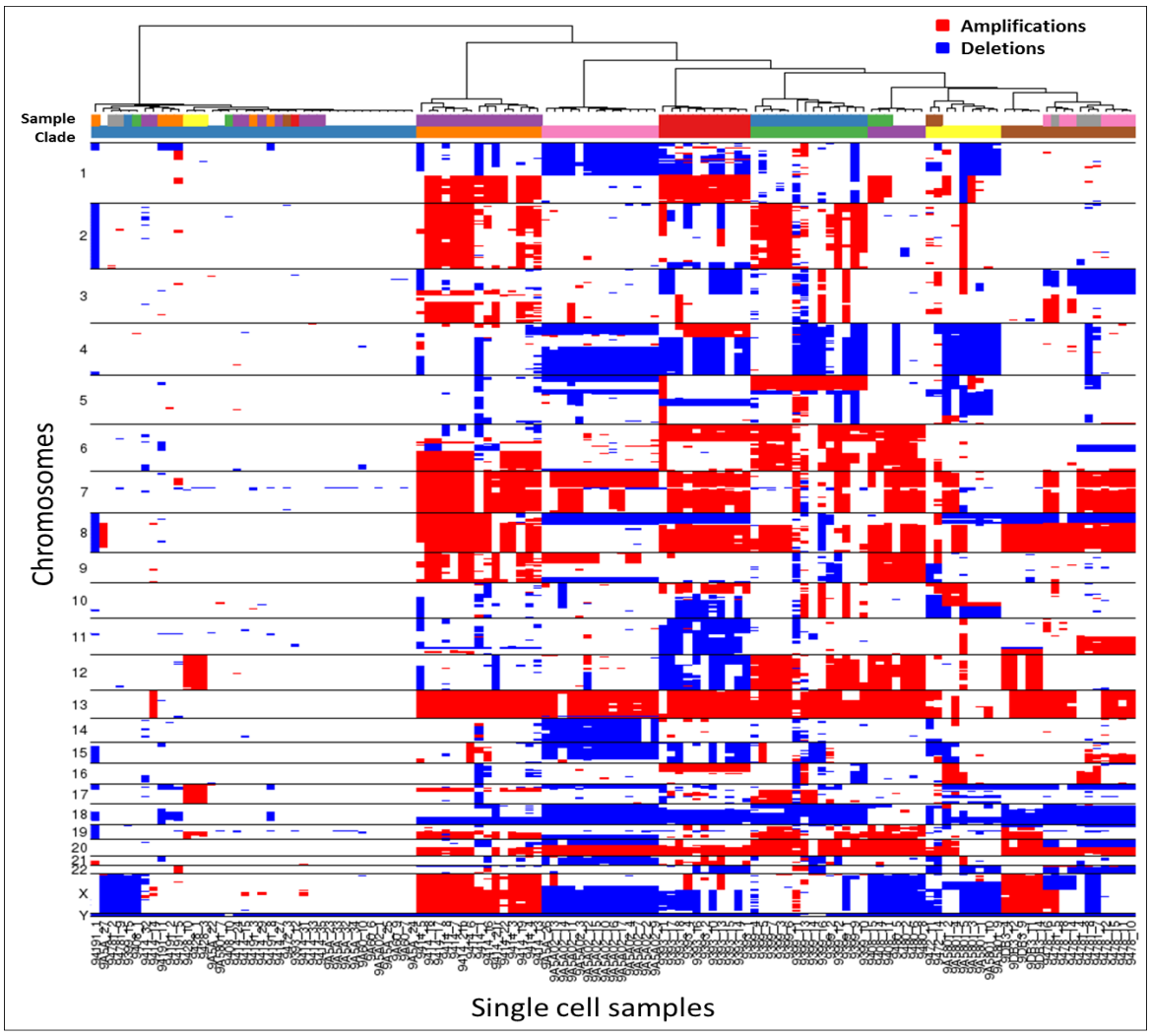

Figure 8: CNV profiles of all analyzed single cells from CRC touch preps. A total of 126 cells isolated from CRC tissue from 12 patients is displayed here in a heatmap (method ‚ward.D', distance method ‚manhattan' with 5k resolution) of 8 clades.

Only patients CRC211 and CRC237 had no clonal cells within their analyzed cells of CRC tissue.

5.6.1 CNV profiles of single cells from hepatic metastases

We analyzed a total of 37 cells from the hepatic metastases of 4 patients and observed clonality within each (100%) of the analyzed patients. Of the 37 cells, 32 (86.5%) were part of clonal profiles. As an example, the heatmap of analyzed cells within the hepatic metastasis of patient CRC205 is displayed in **Figure 9**.

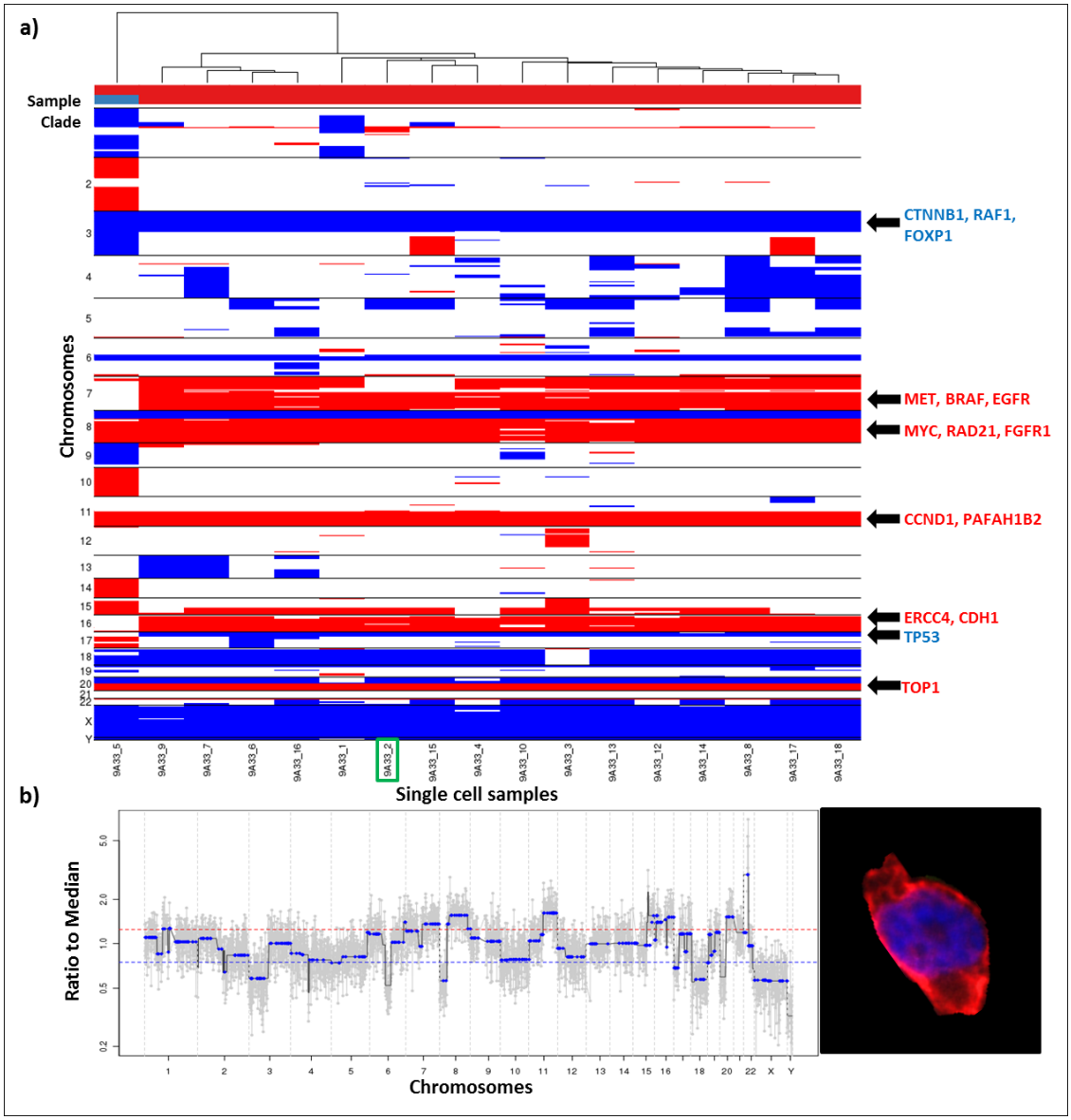

Figure 9: CNV-profiles of 17 cells from a hepatic metastasis of patient CRC205. CNV-profiles of **a)** 17 single-cells from the hepatic metastasis of patient CRC205. 16 cells show clonal profiles and one cell (blue clade) possessing slight s. Marked with a green rectangle is the cell profile displayed in **b)** as a magnification of the clone together with the corresponding composite cell image(red=CK-pan, blue=DAPI and green=CD45). The chosen cell is marked in the heatmap with the green rectangle.

Common amplifications observed were in regions containing *MET*, *BRAF*, *EGFR*, *MYC*, *RAD21*, *CCND1*, *TOP1* and *ERCC4* amongst others. Common deletions were found in regions containing *CTNNB1*, *RAF1*, *FOXP1* and *TP53*.

5.6.4 Comparison of CNV profiles of touch preps and CTCs

We have analzyed CNV profiles of nine pairs of patients with HD-CTCs and matching CRC samples. As no CNV profiles of HD-CTCs were clonal, there was no clonal similarity detectable. The overview of analzyed CNV profiles of isolated single HD-CTCs and single cells from the CRC and hepatic metastasis touch preps from patient CRC205 are displayed in **Figure 10**.

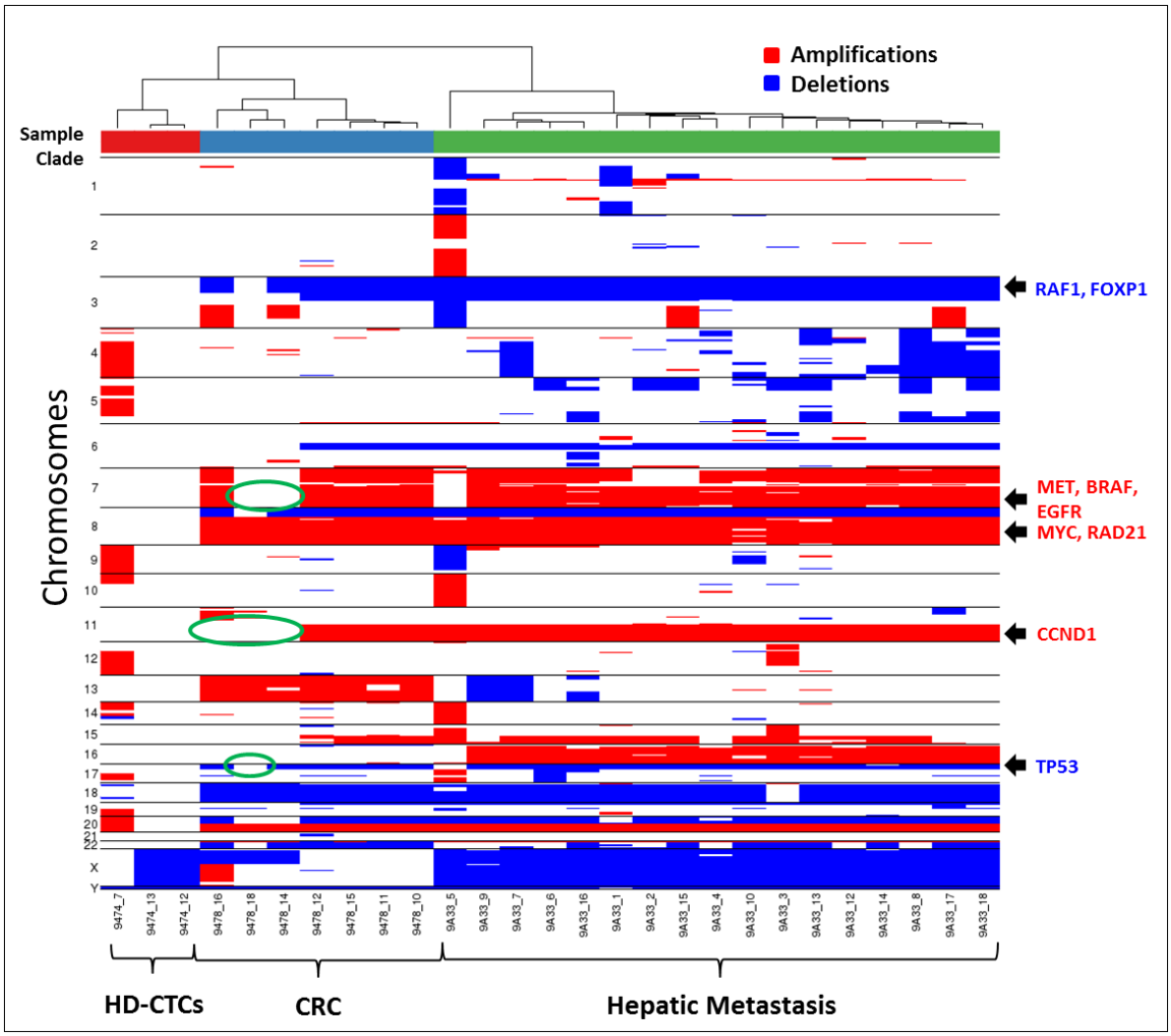

Figure 10: Comparison of CNV profiles of CTCs, single cells from CRC and the hepatic metastasis of patient CRC205. CNV profiles of HD-CTCs (red clade), isolated cells from CRC (blue clade) and the hepatic metastasis (green clade) of patient CRC205. Marked in green are regions within CRC cells that differ from the clone found in the hepatic metastasis.

In direct comparison to profiles from the corresponding CRC cells, the two sources are clustered in different clades and therefore vary. In regard to the overall detected copy number alterations in the three different tumor cell sources, frequencies for altered regions were summarized in **Table 3**.

Table 3: Frequencies for alterations in single cells of three CRC sources

Gene	Function	Type of alteration	CRC	Liver	HD-CTC
MYC	Transcription Factor	Amplification	**43.7%** (55/126)	**83.8%** (31/37)	**0.7%** (1/136)
MET	Proto-Oncogene	Amplification	**37.35%** (47/126)	**67.6%** (25/37)	**1.5%** (2/136)
FGFR1	Growth Factor Receptor	Deletion	**34.9%** (44/126)	**86.5%** (32/37)	**0.7%** (1/136)
CDX2	Transcription Factor	Amplification	**54%** (68/126)	**18.9%** (7/37)	**1.5%** (2/136)
APC	Tumor Suppressor	Deletion	**19.1%** (24/126)	**10.8%** (4/37)	**0%** (0/136)
Polyploidy	—	Numerical change in a whole set of chromosomes	**73.8%** (98/126)	**86.5%** (32/37)	**11%** (15/136)

HD-CTCs showed the lowest frequency in every type of alteration. Within single cells of CRC tissue, 73.8% of cells showed aneuploidy, and 43.7% amplification of the *MYC* region. In liver metastases tissue 86.5% of the cells showed aneuploidy of entire chromosomes and 83.8% showed amplifications of the *MYC* region. Comparing CNVs in CRC tissue to liver tissue showes that alterations in *MYC*, *MET* and *FGFR1* regions increased excessively. Amplification of *CDX2* decreased (from 54% in CRC to 18.9%) and deletion of the *APC* region decreased as well. Alterations of entire chromosomes increased, but only from 73.8% in CRC cells to 86.5% in the liver tissue.

6 Discussion

6.1 Heterogeneity of CTCs in CRC

3001 HD-CTCs were analyzed for nuclear roundness and showed a median value of 0.7, this does not give information about the entire cell, but the nucleus shows elliptical or elongated shapes and the high pleomorphic heterogeneity is conform with results of Ligthart et al. and Marrinucci et al. [48, 49]. For the CTC subcategories, the nuclear roundness was highest for CTC-Small cells and regarding size or nuclear area this category was the most homogenous one. In contrast, the CTC-LowCK category showed the highest heterogeneity regarding nuclear area and one of the highest regarding nuclear roundness. This high heterogeneity in the CTC-LowCK group indicates that it consists of multiple unidentified cell types.

6.2 Enumeration data

6.2.1 HD-CTCs enumeration

Our data showed only 52.2% HD-CTC positive patients in the pre-resection draw. The relatively low CTC positivity rate could be explained through the anatomical position of the colon, which connects the blood vessels of the colon first over the mesenteric and portal vein with the liver, which may function as a sponge for CTCs and could be the reason for the liver being the main metastatic site in CRC [50].

6.2.2 CTC subcategories enumeration

Cells of the other CTC subtypes have been found in many samples, but according to the applied cut-off levels, positivity rate was low. Regarding CTC-LowCK cells, it has been shown before that CTCs can lose epithelial characteristics while undergoing EMT [51]. Therefore, a previous study using the CellSearch® system was perfomed capturing both – $EpCAM^{neg}$ and $EpCAM^{pos}$ cells in metastatic lung cancer patient blood, resulting in a higher overall detection rate of CTCs, but association with poor

outcome was lost for the detected cohort of mixed CTCs compared to only $EpCAM^{pos}$ CTCs [52]. To better understand the COIs we have detected with the HD-SCA platform it will be necessary to apply multivariate analysis to study their phenotypes. Within the Kuhn laboratory tests have been performed using the HYPERION™ imaging system (Fluidigm Corporation, San Francisco, USA) for the detection of over 30 protein markers in parallel in one cell [53]. This allows detection tissue specific or therapy relevant as well as markers for EMT, stemness and other disease evolution relevant markers on the HD-SCA platform. Besides, it will give insight into HD-CTCs, cells of the CTC subcategories and CTCCs, but also allow characterization of the patient's immune signature.

6.2.3 CTCC enumeration

Our cohort had a relatively low CTCC count (39.1% positive pateints in pre-resection) compared to cluster counts in previously published studies. CTCC positivity rates in CRC patients have been as high as 68.8% in a study with 32 patients of different stages [54]. Cima et al. showed in 2016 that $CD45^{neg}$ -cell clusters (isolated from CRC patients through use of a microfiltration device in combination with immunofluorescent staining) expressing CK (CK8 and CK20), but no EpCAM are actually tumor derived endothelial cell clusters [55]. This could also be the case in our results. However, even the detected endothelial cell clusters have only been present in CRC patients and not in healthy volunteers just as in our cohort.

6.4 Survival analysis

6.4.1 Association of clinical characteristics with survival

Our results are conform with previously published data that right sided metastatic CRC is associated with shorter OS [56]. The worst prognosis in our cohort was detected for patients with transverse CRC. Studies usually separate the colon only in two locations; counting the transverse colon as right-sided CRC. Our results show that probably the differentiation of the transverse colon may be a valuable prognostic

information. Overall, the correlations between primary tumor size and amount of hepatic metastases with OS is in agreement with the literature [57, 58].

6.4.2 Association of HD-CTCs with survival

CTC enumeration has been established as a predictive and prognostic marker for PFS and OS in metastatic CRC [59–61]. These findings were mainly established using the CellSearch® platform, which is based on detection of EpCAM positive cells. Interestingly, our results are not conforming to these findings. This might be caused by the CTC detection method. So far, there are limited reports regarding CTCs detected in metastatic CRC patients by non-enrichment techniques. Another important and often ignored fact is, that circulating endothelial cells (CECs) are often increased in cancer patients [62], and it has been shown that CECs are expressing keratins similar to epithelia [63]. Therefore we cannot exclude the possibility of detecting a mixed population of CECs and CTCs. This CTC mixture could be similar to cells detected in the previously mentioned CellSearch® study where this mixed population of $EpCAM^{pos}$ and $EpCAM^{neg}$ cells was also not correlated to survival [52].

To distinguish between CECs and HD-CTCs, the HD-SCA workflow has recently been adjusted and the platelet endothelial cell adhesion molecule marker CD31 has been added to the workflow. This will allow future analysis of both populations seperately.

6.4.3 Association of CTC subcategories with survival

As the only CTC subcategory with association to OS and PFS, CTC-Small cells may represent the cell population usually detected by EpCAM-based techniques. Morphological characteristics of published data of CECs [64, 65] mostly resemble the detected HD-CTC category. The CTC-Small category possessed the highest roundness in our cohort (**Figure 2**) and this morphology is often displayed in papers as CTC properties associated to cancer patient survival [66]. In the study of Ligthart et al. it was discovered that higher counts of CTCs and CTCs with a roundness close to one are more dangerous for the patient than elongated cells, also that small CTCs in breast cancer are more dangerous than large CTCs [49]. This confirms our findings

that the CTC-Small subcategory might be the CTC population with the highest importance for disease development.

As the CTC-LowCK cells are defined as CK^{neg} and $CD45^{neg}$ they might be similar to the $EpCAM^{neg}$ cells detected in the CellSearch® study, which could explain their missing association to patient survival. The major issue with this cell category is that there is not enough information about what particular cell type is forming this group and it is highly possible that it consists of cells of various origins. To answer this question, experiments with multiplex protein analysis will be used to further characterize the CTC-LowCK phenotype.

6.4.4 Association of CTCCs with survival

Based on our results, the size of CTCCs is associated to OS. As only three patients possessed clusters larger than 8 cells, more data should be acquired before reliable conclusions can be drawn. Other publications have observed CTCCs in breast, prostate or lung cancer and identified CTCCs as promising markers of survival, sometimes exceeding CTCs [67, 68]. This might be linked to the possibility that CTCCs might act as metastatic drivers.

The higher metastatic potential and chance of survival of CTCCs may be caused by their close association to other cell types as fibroblasts, platelets and endothelial cells [39]. Therefore a large CTCC may just bring their own “soil” and enhance the potential to extravasate and then proliferate in distant tissue [69].

6.5 Association of enumeration data with clinical characteristics

6.5.1 Association of HD-CTCs with clinical characteristics

In our data the transverse colon CRC has been associated with shedding the most HD-CTCs/ml in the pre-resection draw. The increased exposure to movement and presence of multiple blood supplies may cause tumors in this area to shed a larger amount of cells, which is supported by many reports stating higher numbers of CTCs in right-sided CRC [70]. HD-CTC counts have also been significantly higher in patients

with *KRAS* mutated tumors. As *KRAS* is a GTPase that acts as a switch for signaling networks associated to cell differentiation, survival, migration and growth, it plays a large role in CRC development and is a regulator of EMT [70, 71]. As EMT has been proposed as one of the major contributors to tumor cell intravasation into the vasculature [72], higher HD-CTC counts in *KRAS* mutated tumors could be the consequence. And as discussed before, evidence suspects that HD-CTCs may also represent CECs in the bloodstream.

HD-CTCs have been the only category of cells that significantly decreased in numbers after resection of the primary tumor. The primary tumor may be the main source of HD-CTCs in CRC stage IV patients.

6.5.2 Association of CTC subcategories with clinical characteristics

CTC-Small cells in the pre-resection draws were significantly higher in patients with *KRAS* mutated tumors. This evidence might show a close connection to HD-CTCs or rather that *KRAS* mutated tumors may have more disrupted capillary walls caused by cells of a more mobile and mesenchymal phenotype, therefore releasing more CECs and CTCs [72]. Cells of the CTC-LowCK category were, like HD-CTCs, also more prevalent in transverse CRC. This extensive shedding may be caused by the same reasons as discussed for HD-CTCs, related to the exposed anatomical position of the transverse colon.

6.5.3 Association of CTCCs with clinical characteristics

The amount of cells in a CTCC was significantly higher in M1 patients compared to M0 and the amount of detected CTCCs has been significantly higher in *KRAS* mutated patients. These findings support the theory that clusters are related to highly chromosomal instable CRC as the *KRAS* mutation is one of the key events in the development of CIN in CRC [73]. Also M1 status patients have been diagnosed with synchronous disease which implies that the disease load developed over a longer time without detection and the tumor might have had more time to gain higher CIN. CTCCs were shown to be strongly associated with hepatic metastases, but data is not

sufficient enough to conclude if they are causing hepatic metastases or rather originate from them. One promising tool will be the use of multiplex protein detection by using the HYPERION™ technique [53].

6.6 CNV profiles

Clonal profiles within detected CTCs have been reported for prostate cancer [74], breast cancer [75], melanoma [76] and lung cancer [77]. Often clonal development was able to uncover temporal disease development and acquisition of amplifications.

6.6.1 CNV profiles of HD-CTCs

In our data, clonality in HD-CTCs was neither detected within individual patients, nor amongst cells of all analyzed 11 patients. One reason may be the fact that the captured cells have passed through the liver and are collected from peripheral blood. Therefore CTCs with acquired major alterations may have already seeded in the liver. On the other hand these findings are supporting the aforementioned theory that the detected group of HD-CTCs are representing tumor derived CECs. This cell type has been analyzed by Cima et al. and did not mirror mutations and chromosomal abnormalities of the primary tumor [55]. Further analyses, using CD31 as additional fluorescence marker or multiplex protein detection are prepared to answer this question.

6.6.2 CNV profiles in tissue samples compared to those of HD-CTCs

Common alteration have been observed within the CRC tissue cells of one patient as well as within cells isolated from multiple patients. Amplifications of similar regions have been observed in 43.7% of cells and numerical changes in a whole set of chromosomes even in 73.8% of cells from CRC tissue. As CRC tumors share common pathways of molecular development, common alterations within the genome could be expected. But as tumor tissue is composed of multiple associated cell types as macrophages [78], stromal cells [79] and endothelial cells [80], some cells analyzed

without showing clonal or altered CNV profiles may belong to one of these tumor associated cell categories. Based on our data there is a high similarity between CNV profiles of CRC tissue cells and cells isolated from hepatic metastases. In addition, a clear evolution from the primary tumor to metastasis is visible when special regions are analyzed. As we had access to CTCs in the blood and tumor cells from tissue, we aimed to link clones from the tissue to CTC phenotype associated to the hepatic metastases, but could not find any clonality in the blood. For proper statistical comparison of clones in the primary tumor to those in hepatic metastases the sample size was too small, but it became one of the goals for a future project.

7 Conclusions

Based on our data it is most likely that the detected category of HD-CTCs in CRC consists of mostly tumor associated CECs. This was backed by the results of our CNV data. In contrast, the CTC subcategory of CTC-Small cells showed morphology and association to OS, as typical CTCs do. Results for detected CTCCs were most interesting, showing that size matters. The number of cells per CTCC was associated to OS and significantly elevated in M1 CRC patients. The number of CTCCs/ml was significantly elevated in the pre-resection draws of *KRAS* mutated CRCs. This makes CTCCs a promising biomarker for CRC patients and a probable driver of metastasation. The detected category of HD-CTCs has to be analyzed for endothelial origin. For further enumeration studies we would apply the updated HD-SCA detection with CD31 signal inclusion. As the analysis of association with survival was successful in the category of CTC-Small cells, these cells should be in the focus of future studies. The use of CK markers instead of EpCAM might be an obstacle due to parallel expression in endothelial cells. Regarding the detected CTCCs, we would focus in future projects on their multiplex profiling to decipher protein expression and the cell phenotypes of individual cells assembling a CTCC.

8 Literature

1. Malvezzi M, Carioli G, Bertuccio P, et al (2017) European cancer mortality predictions for the year 2017, with focus on lung cancer. Ann Oncol 28:1117–1123 . doi: 10.1093/annonc/mdx033

2. Ait Ouakrim D, Pizot C, Boniol M, et al (2015) Trends in colorectal cancer mortality in Europe: retrospective analysis of the WHO mortality database. BMJ h4970 . doi: 10.1136/bmj.h4970

3. Ferlay J, Steliarova-Foucher E, Lortet-Tieulent J, et al (2013) Cancer incidence and mortality patterns in Europe: Estimates for 40 countries in 2012. Eur J Cancer 49:1374–1403 . doi: 10.1016/j.ejca.2012.12.027

4. Brenner H, Hoffmeister M, Brenner G, et al (2009) Expected reduction of colorectal cancer incidence within 8 years after introduction of the German screening colonoscopy programme: Estimates based on 1,875,708 screening colonoscopies. Eur J Cancer 45:2027–2033 . doi: 10.1016/j.ejca.2009.02.017

5. Brenner H, Stock C, Hoffmeister M (2014) Effect of screening sigmoidoscopy and screening colonoscopy on colorectal cancer incidence and mortality: systematic review and meta-analysis of randomised controlled trials and observational studies. BMJ 348:g2467–g2467 . doi: 10.1136/bmj.g2467

6. Kang H, Shibata D (2013) Direct Measurements of Human Colon Crypt Stem Cell Niche Genetic Fidelity: The Role of Chance in Non-Darwinian Mutation Selection. Front Oncol 3: . doi: 10.3389/fonc.2013.00264

7. Grady WM, Markowitz SD (2015) The Molecular Pathogenesis of Colorectal Cancer and Its Potential Application to Colorectal Cancer Screening. Dig Dis Sci 60:762–772 . doi: 10.1007/s10620-014-3444-4

8. Weinberg RA (2014) The biology of cancer, Second edition. Garland Science, Taylor & Francis Group, New York

9. Armaghany T, Wilson JD, Chu Q, Mills G (2012) Genetic alterations in colorectal cancer. Gastrointest Cancer Res GCR 5:19–27

10. Grady WM (2004) Genomic instability and colon cancer. Cancer Metastasis Rev 23:11–27

11. Geiersbach KB, Samowitz WS (2011) Microsatellite Instability and Colorectal Cancer. Arch Pathol Lab Med 135:1269–1277 . doi: 10.5858/arpa.2011-0035-RA

12. Parsons MT, Buchanan DD, Thompson B, et al (2012) Correlation of tumour BRAF mutations and *MLH1* methylation with germline mismatch repair (MMR) gene mutation status: a literature review assessing utility of tumour features for MMR variant classification. J Med Genet 49:151–157 . doi: 10.1136/jmedgenet-2011-100714

13. Kinzler KW, Vogelstein B (1996) Lessons from hereditary colorectal cancer. Cell 87:159–170

14. Ma H, Brosens LAA, Offerhaus GJA, et al (2018) Pathology and genetics of hereditary colorectal cancer. Pathology (Phila) 50:49–59 . doi: 10.1016/j.pathol.2017.09.004

15. Zavoral M, Suchanek S, Zavada F, et al (2009) Colorectal cancer screening in Europe. World J Gastroenterol 15:5907–5915

16. What Are the Survival Rates for Colorectal Cancer, by Stage? https://www.cancer.org/cancer/colon-rectal-cancer/detection-diagnosis-staging/survival-rates.html. Accessed 2 Feb 2018

17. Lieberman DA (2009) Screening for Colorectal Cancer. N Engl J Med 361:1179–1187 . doi: 10.1056/NEJMcp0902176

18. Thomas DS, Fourkala E-O, Apostolidou S, et al (2015) Evaluation of serum CEA, CYFRA21-1 and CA125 for the early detection of colorectal cancer using longitudinal preclinical samples. Br J Cancer 113:268–274 . doi: 10.1038/bjc.2015.202

19. Mondal S, Sinha S, Mukhopadhyay M, et al (2014) Diagnostic and prognostic significance of different mucin expression, preoperative CEA, and CA-125 in colorectal carcinoma: A clinicopathological study. J Nat Sci Biol Med 5:404 . doi: 10.4103/0976-9668.136207

20. Shaib W, Mahajan R, El-Rayes B (2013) Markers of resistance to anti-EGFR therapy in colorectal cancer. J Gastrointest Oncol 4:308–318 . doi: 10.3978/j.issn.2078-6891.2013.029

21. Kufe DW, Holland JF, Frei E, American Cancer Society (2003) Cancer medicine 6, 6th ed. BC Decker, Hamilton, Ont. ; Lewiston, NY

22. Colon Cancer Treatment. In: Natl. Cancer Inst. https://www.cancer.gov/types/colorectal/hp/colon-treatment-pdq#section/_105. Accessed 19 Apr 2018

23. Gasch C, Plummer PN, Jovanovic L, et al (2015) Heterogeneity of miR-10b expression in circulating tumor cells. Sci Rep 5:15980 . doi: 10.1038/srep15980

24. Schramm A, Friedl TWP, Schochter F, et al (2016) Therapeutic intervention based on circulating tumor cell phenotype in metastatic breast cancer: concept of the DETECT study program. Arch Gynecol Obstet 293:271–281 . doi: 10.1007/s00404-015-3879-7

25. Shaw Bagnall J, Byun S, Begum S, et al (2015) Deformability of Tumor Cells versus Blood Cells. Sci Rep 5:18542 . doi: 10.1038/srep18542

26. Kalluri R, Weinberg RA (2009) The basics of epithelial-mesenchymal transition. J Clin Invest 119:1420–1428 . doi: 10.1172/JCI39104

27. Liu Z-J, Semenza GL, Zhang H-F (2015) Hypoxia-inducible factor 1 and breast cancer metastasis. J Zhejiang Univ Sci B 16:32–43 . doi: 10.1631/jzus.B1400221

28. Yeo CD, Kang N, Choi SY, et al (2017) The role of hypoxia on the acquisition of epithelial-mesenchymal transition and cancer stemness: a possible link to epigenetic regulation. Korean J Intern Med 32:589–599 . doi: 10.3904/kjim.2016.302

29. Hazan RB, Qiao R, Keren R, et al (2004) Cadherin switch in tumor progression. Ann N Y Acad Sci 1014:155–163

30. Martin TA, Ye L, Sanders AJ, et al (2013) Cancer Invasion and Metastasis: Molecular and Cellular Perspective. In: Metastatic Cancer: Clinical and Biological Perspectives. Landes Bioscience

31. Chang JT, Mani SA (2013) Sheep, wolf, or werewolf: Cancer stem cells and the epithelial-to-mesenchymal transition. Cancer Lett 341:16–23 . doi: 10.1016/j.canlet.2013.03.004

32. Shibue T, Brooks MW, Weinberg RA (2013) An Integrin-Linked Machinery of Cytoskeletal Regulation that Enables Experimental Tumor Initiation and Metastatic Colonization. Cancer Cell 24:481–498 . doi: 10.1016/j.ccr.2013.08.012

33. Tian X, Liu Z, Niu B, et al (2011) E-Cadherin/ β -Catenin Complex and the Epithelial Barrier. J Biomed Biotechnol 2011:1–6 . doi: 10.1155/2011/567305

34. Bedke J, Heide J, Ribback S, et al (2018) Microvascular and lymphovascular tumour invasion are associated with poor prognosis and metastatic spread in renal cell carcinoma: a validation study in clinical practice. BJU Int 121:84–92 . doi: 10.1111/bju.13984

35. Lim S-B, Yu CS, Jang SJ, et al (2010) Prognostic Significance of Lymphovascular Invasion in Sporadic Colorectal Cancer: Dis Colon Rectum 53:377–384 . doi: 10.1007/DCR.0b013e3181cf8ae5

36. Zhe X, Cher ML, Bonfil RD (2011) Circulating tumor cells: finding the needle in the haystack. Am J Cancer Res 1:740–751

37. Yao D, Dai C, Peng S (2011) Mechanism of the Mesenchymal-Epithelial Transition and Its Relationship with Metastatic Tumor Formation. Mol Cancer Res 9:1608–1620 . doi: 10.1158/1541-7786.MCR-10-0568

38. Cristofanilli M, Hayes DF, Budd GT, et al (2005) Circulating tumor cells: a novel prognostic factor for newly diagnosed metastatic breast cancer. J Clin Oncol Off J Am Soc Clin Oncol 23:1420–1430 . doi: 10.1200/JCO.2005.08.140

39. Thiele J-A, Bethel K, Králíčková M, Kuhn P (2017) Circulating Tumor Cells: Fluid Surrogates of Solid Tumors. Annu Rev Pathol Mech Dis 12:419–447 . doi: 10.1146/annurev-pathol-052016-100256

40. Baker MK, Mikhitarian K, Osta W, et al (2003) Molecular detection of breast cancer cells in the peripheral blood of advanced-stage breast cancer patients using multimarker real-time reverse transcription-polymerase chain reaction and a novel porous barrier density gradient centrifugation technology. Clin Cancer Res Off J Am Assoc Cancer Res 9:4865–4871

41. Chinen LTD, de Carvalho FM, Rocha BMM, et al (2013) Cytokeratin-based CTC counting unrelated to clinical follow up. J Thorac Dis 5:593–599 . doi: 10.3978/j.issn.2072-1439.2013.09.18

42. Marrinucci D, Bethel K, Kolatkar A, et al (2012) Fluid biopsy in patients with metastatic prostate, pancreatic and breast cancers. Phys Biol 9:016003 . doi: 10.1088/1478-3975/9/1/016003

43. Heitzer E, Auer M, Gasch C, et al (2013) Complex tumor genomes inferred from single circulating tumor cells by array-CGH and next-generation sequencing. Cancer Res 73:2965–2975 . doi: 10.1158/0008-5472.CAN-12-4140

44. Alix-Panabieres C, Pantel K (2016) Clinical Applications of Circulating Tumor Cells and Circulating Tumor DNA as Liquid Biopsy. Cancer Discov. doi: 10.1158/2159-8290.CD-15-1483

45. Malihi PD, Morikado M, Welter L, et al (2018) Clonal diversity revealed by morphoproteomic and copy number profiles of single prostate cancer cells at diagnosis. Converg Sci Phys Oncol 4:015003 . doi: 10.1088/2057-1739/aaa00b

46. Baslan T, Kendall J, Rodgers L, et al (2012) Genome-wide copy number analysis of single cells. Nat Protoc 7:1024–1041 . doi: 10.1038/nprot.2012.039

47. Thiele J-A, Bethel K, Králíčková M, Kuhn P (2017) Circulating Tumor Cells: Fluid Surrogates of Solid Tumors. Annu Rev Pathol Mech Dis 12:419–447 . doi: 10.1146/annurev-pathol-052016-100256

48. Marrinucci D, Bethel K, Lazar D, et al (2010) Cytomorphology of Circulating Colorectal Tumor Cells: A Small Case Series. J Oncol 2010:1–7 . doi: 10.1155/2010/861341

49. Ligthart ST, Coumans FAW, Bidard F-C, et al (2013) Circulating Tumor Cells Count and Morphological Features in Breast, Colorectal and Prostate Cancer. PLoS ONE 8:e67148 . doi: 10.1371/journal.pone.0067148

50. Sheth KR, Clary BM (2005) Management of Hepatic Metastases from Colorectal Cancer. Clin Colon Rectal Surg 18:215–223 . doi: 10.1055/s-2005-916282

51. Hyun K-A, Koo G-B, Han H, et al (2016) Epithelial-to-mesenchymal transition leads to loss of EpCAM and different physical properties in circulating tumor cells from metastatic breast cancer. Oncotarget 7: . doi: 10.18632/oncotarget.8250

52. Wit S de, Dalum G van, Lenferink ATM, et al (2015) The detection of EpCAM+ and EpCAM– circulating tumor cells. Sci Rep 5:12270

53. Gerdtsson E, Pore M, Thiele J-A, et al (2018) Multiplex protein detection on circulating tumor cells from liquid biopsies using imaging mass cytometry. Converg Sci Phys Oncol 4:015002 . doi: 10.1088/2057-1739/aaa013

54. Molnar B, Ladanyi A, Tanko L, et al (2001) Circulating tumor cell clusters in the peripheral blood of colorectal cancer patients. Clin Cancer Res Off J Am Assoc Cancer Res 7:4080–4085

55. Cima I, Kong SL, Sengupta D, et al (2016) Tumor-derived circulating endothelial cell clusters in colorectal cancer. Sci Transl Med 8:345ra89-345ra89 . doi: 10.1126/scitranslmed.aad7369

56. Boeckx N, Koukakis R, Op de Beeck K, et al (2017) Primary tumor sidedness has an impact on prognosis and treatment outcome in metastatic colorectal cancer: results from two randomized first-line panitumumab studies. Ann Oncol 28:1862–1868 . doi: 10.1093/annonc/mdx119

57. Saha S, Shaik M, Johnston G, et al (2015) Tumor size predicts long-term survival in colon cancer: an analysis of the National Cancer Data Base. Am J Surg 209:570–574 . doi: 10.1016/j.amjsurg.2014.12.008

58. Engstrand J, Nilsson H, Strömberg C, et al (2018) Colorectal cancer liver metastases – a population-based study on incidence, management and survival. BMC Cancer 18: . doi: 10.1186/s12885-017-3925-x

59. Cohen SJ, Punt CJA, Iannotti N, et al (2008) Relationship of circulating tumor cells to tumor response, progression-free survival, and overall survival in patients with metastatic colorectal cancer. J Clin Oncol Off J Am Soc Clin Oncol 26:3213–3221 . doi: 10.1200/JCO.2007.15.8923

60. Groot Koerkamp B, Rahbari NN, Büchler MW, et al (2013) Circulating Tumor Cells and Prognosis of Patients with Resectable Colorectal Liver Metastases or Widespread Metastatic Colorectal Cancer: A Meta-Analysis. Ann Surg Oncol 20:2156–2165 . doi: 10.1245/s10434-013-2907-8

61. Matsusaka S, Suenaga M, Mishima Y, et al (2011) Circulating tumor cells as a surrogate marker for determining response to chemotherapy in Japanese patients with metastatic colorectal cancer. Cancer Sci 102:1188–1192 . doi: 10.1111/j.1349-7006.2011.01926.x

62. Beerepoot LV, Mehra N, Vermaat JSP, et al (2004) Increased levels of viable circulating endothelial cells are an indicator of progressive disease in cancer patients. Ann Oncol 15:139–145 . doi: 10.1093/annonc/mdh017

63. Miettinen M, Fetsch JF (2000) Distribution of keratins in normal endothelial cells and a spectrum of vascular tumors: Implications in tumor diagnosis. Hum Pathol 31:1062–1067 . doi: 10.1053/hupa.2000.9843

64. Bethel K, Luttgen MS, Damani S, et al (2014) Fluid phase biopsy for detection and characterization of circulating endothelial cells in myocardial infarction. Phys Biol 11:016002 . doi: 10.1088/1478-3975/11/1/016002

65. Rigolin GM (2006) Neoplastic circulating endothelial cells in multiple myeloma with 13q14 deletion. Blood 107:2531–2535 . doi: 10.1182/blood-2005-04-1768

66. Hardingham JE, Grover P, Winter M, et al (2015) Detection and Clinical Significance of Circulating Tumor Cells in Colorectal Cancer--20 Years of Progress. Mol Med Camb Mass 21 Suppl 1:S25-31 . doi: 10.2119/molmed.2015.00149

67. Zurita AJ, Carlsson A, Troncoso P, et al (2016) Abstract 4966: High-definition single cell analysis (HD-SCA) reveals enrichment in androgen receptor (AR) expression in tumor cell clusters in bone marrow and blood

of metastatic castration-resistant prostate cancer (mCRPC) patients. Cancer Res 76:4966–4966 . doi: 10.1158/1538-7445.AM2016-4966

68. Carlsson A, Nair VS, Luttgen MS, et al (2014) Circulating Tumor Microemboli Diagnostics for Patients with Non–Small-Cell Lung Cancer. J Thorac Oncol 9:1111–1119 . doi: 10.1097/JTO.0000000000000235

69. Ribatti D, Mangialardi G, Vacca A (2006) Stephen Paget and the 'seed and soil' theory of metastatic dissemination. Clin Exp Med 6:145–149 . doi: 10.1007/s10238-006-0117-4

70. Arnold D, Lueza B, Douillard J-Y, et al (2017) Prognostic and predictive value of primary tumour side in patients with RAS wild-type metastatic colorectal cancer treated with chemotherapy and EGFR directed antibodies in six randomized trials†. Ann Oncol 28:1713–1729 . doi: 10.1093/annonc/mdx175

71. Shelygin YA, Pospekhova NI, Shubin VP, et al (2014) Epithelial-Mesenchymal Transition and Somatic Alteration in Colorectal Cancer with and without Peritoneal Carcinomatosis. BioMed Res Int 2014:1–7 . doi: 10.1155/2014/629496

72. Thiery JP (2002) Epithelial–mesenchymal transitions in tumour progression. Nat Rev Cancer 2:442–454 . doi: 10.1038/nrc822

73. Pino MS, Chung DC (2010) The Chromosomal Instability Pathway in Colon Cancer. Gastroenterology 138:2059–2072 . doi: 10.1053/j.gastro.2009.12.065

74. Dago AE, Stepansky A, Carlsson A, et al (2014) Rapid Phenotypic and Genomic Change in Response to Therapeutic Pressure in Prostate Cancer Inferred by High Content Analysis of Single Circulating Tumor Cells. PLoS ONE 9:e101777 . doi: 10.1371/journal.pone.0101777

75. Neves RPL, Raba K, Schmidt O, et al (2014) Genomic High-Resolution Profiling of Single CKpos/CD45neg Flow-Sorting Purified Circulating Tumor Cells from Patients with Metastatic Breast Cancer. Clin Chem. doi: 10.1373/clinchem.2014.222331

76. Ruiz C, Li J, Luttgen MS, et al (2015) Limited genomic heterogeneity of circulating melanoma cells in advanced stage patients. Phys Biol 12:016008 . doi: 10.1088/1478-3975/12/1/016008

77. Ni X, Zhuo M, Su Z, et al (2013) Reproducible copy number variation patterns among single circulating tumor cells of lung cancer patients. Proc Natl Acad Sci U S A 110:21083–21088 . doi: 10.1073/pnas.1320659110

78. Noy R, Pollard JW (2014) Tumor-Associated Macrophages: From Mechanisms to Therapy. Immunity 41:49–61 . doi: 10.1016/j.immuni.2014.06.010

79. Bussard KM, Mutkus L, Stumpf K, et al (2016) Tumor-associated stromal cells as key contributors to the tumor microenvironment. Breast Cancer Res 18: . doi: 10.1186/s13058-016-0740-2

80. Dudley AC (2012) Tumor Endothelial Cells. Cold Spring Harb Perspect Med 2:a006536–a006536 . doi: 10.1101/cshperspect.a006536

9 Publications

A summary of all composed publications regarding this thesis and projects executed during the time of this work are listed here and attached in the following order within chapter 9:

I. Circulating Tumor Cells: Fluid Surrogates of Solid Tumors; Review

Thiele J-A, Bethel K, Králíčková M, Kuhn P, 2017, Circulating Tumor Cells: Fluid Surrogates of Solid Tumors. Annu Rev Pathol Mech Dis 12:419–447. doi: 10.1146/annurev-pathol-052016-100256 **(IF_{2017} = 15.95)**

II. Multiplex protein detection on circulating tumor cells from liquid biopsies using imaging mass cytometry; Research Article

Gerdtsson E, Pore M, Thiele J-A, et al., 2018, Multiplex protein detection on circulating tumor cells from liquid biopsies using imaging mass cytometry. Converg Sci Phys Oncol 4:015002. doi: 10.1088/2057-1739/aaa013

(Journal has recently been selected for indexing in Clarivate Analytics Emerging Sources Citation Index (ESCI); listed in Web of Science as of next year).

III. Single-Cell Analysis of Circulating Tumor Cells; Book chapter

Thiele J-A, Pitule P, Hicks J and Kuhn P., Single-Cell Analysis of Circulating Tumor Cells. Methods Mol Biol., accepted in March 2018.

(Scopus cite $score_{2017}$ = 0.96)

IV. lncRNAs in healthy tissue have prognostic value in colorectal cancer; Research Article

Thiele J-A, Hosek P, Kralovcova E, Ostasov P, Liska V, Bruha J, Vycital O, Rosendorf J, Kralickova M, Pitule P, lncRNAs in healthy tissue have prognostic value in colorectal cancer, Submitted to BMC Cancer: June 2018 **(IF_{2017} = 3.28)**